An Efficient Electrocatalyst for the Nano-Level Detection of Neurotransmitter (Dopamine) in Biologic Matrices based on Samarium (III) Oxide Nanoparticles; An Electrochemical Approaches

Elayappan Tamilalagan[1],†, Tse-Wei Chen[2,3],†, Shen-Ming Chen[1,], Muthumariappan Akilarasan[1], Yi-Chen Huang[1], Syang-Peng Rwei[3,4]*

[1] Department of Chemical Engineering and Biotechnology, National Taipei University of Technology, Taipei, Taiwan 106 (ROC).
[2] Department of Materials, Imperial College London, London, SW7 2AZ, United Kingdom
[3] Research and Development Center for Smart Textile Technology, National Taipei University of Technology, Taiwan
[4] Institute of Organic and Polymeric Materials, National Taipei University of Technology,
[*]E-mail: smchen78@ms15.hinet.net
†Authors contributed equally.

Dopamine (DA) play a vital role in brain as a neurotransmitter and its excess secretion can leads to several abnormalities. The important challenge in DA detection was the existence of interference like ascorbic acid and uric acid in blood. Therefore, it is important to improve the selective and sensitive detection of DA in biological samples. Herein, we reported the synthesis of samarium oxide (Sm_2O_3) nanoparticle for the selective detection of DA. The morphological and chemical composition of the as prepared Sm_2O_3 NPs was characterized by using FESEM and XRD. In addition, the synthesized Sm_2O_3 NPs were modified on the GCE surface, which was subjected for the determination of DA. Moreover, the Sm_2O_3 NPs/GCE has displayed the wider covering range of 0.01 to 342.9 µM with limit of detection up to 2.54 nM. The Sm_2O_3 NPs/GCE were successfully examined with DA spiked human blood serum and urine samples, which shows the appreciable found and recovery values.

1. INTRODUCTION

Dopamine (DA) is one of the most important neurotransmitter, which plays major role in the function of mammalian neuronal networks[1, 2]. Dopamine is also used as an adrenergic in feedstuff

especially in the lean meat powder, which help animals to gain muscles rather than fat[3]. Hence, the usage of dopamine as an adrenergic in feedstuff has been banned in various countries[4]. However, the illegal usage of dopamine as an adrenergic may enters into human food chain and causes several health risks[5]. The abnormal level of dopamine in the human metabolism may causes severe health effects such as schizophrenia[6], and Parkinson's disease[7]. Therefore, it is essential to develop an accuracy method to detect the DA in biological fluids. There are various analytical methods has been proposed to detect the DA but the electrochemical techniques are considering as the promising method due its rapid detection, require less analysis time and high selectivity[8, 9]. However, using the unmodified electrodes for the biomolecules detection provides low sensitivity and selectivity[10]. Therefore, it is necessary to discover the new electrode materials with high efficiency for the electrochemical detection of DA.

In recent nanostructured, metal oxides have been widely used in the field of electrochemical sensors, supercapacitors, and solar cell applications [11, 12]. Generally, transition metal oxides have been investigated more in the field of electrochemical sensor compare with rare earth metal oxide[13, 14]. However, the rare earth metals have some unique properties such as providing larger surface area, less size, and interfacial effects[15]. Among them samarium oxide plays vital role in the electrochemical application due to its high dielectric constant[16]. Furthermore, the samarium oxides holds the excellent band gap of 4.33 eV and significant refractive index of 1.93[16]. Thus, considering the unique properties of Sm_2O_3 we have developed the electrochemical sensor based on the Sm_2O_3.
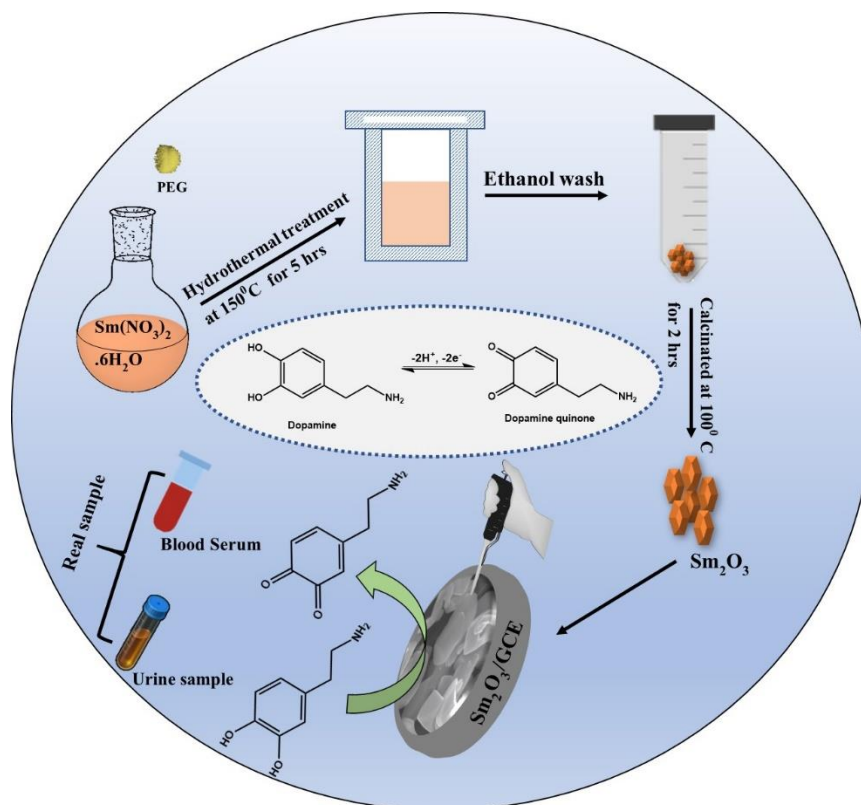
Scheme 1. A visual illustration of Synthesis of Sm_2O_3 NPs and its electrochemical detection of DA

Herein, we reported the efficient electrochemical sensor based on the Sm_2O_3 NPs for the detection of DA in biological fluids. The Sm_2O_3 NPs modified nanomaterials shows the excellent charger

transfer resistance of R_{ct} of the 87.46 Ω. Furthermore, the Sm_2O_3 NPs/GCE significantly improved the electro oxidation of dopamine. Finally, the as prepared sensor shows the outstanding performance in the real samples such as human blood serum and urine samples.

2. EXPERIMENTAL SECTION

2.1. Materials and Methods

Double distilled water was used for all the experiments. 0.1 M phosphate buffer (PB) (pH 7.0) prepared from sodium dihydrogen phosphate and disodium hydrogen phosphate was used as supporting electrolyte. The surface modification of the as-formed composite was probed using field emission scanning electron microscope (FESEM-JEOL-7600F). PerkinElmer PHI-5702 investigated the quantitative analysis, defects, and disorder nature of the as-prepared composite and the crystallinity nature of the composite was examined through the XRD, XPERT-PRO spectrometer (PANalytical B.V.). The electrochemical property and electrocatalytic activity was scrutinized using electrochemical impedance spectroscopy (EIS), and cyclic voltammetry (CV), and DPV were carried out CHI 1205A. The CHI instrument consist on three electrodes system, whereas, the platinum wire and Ag/AgCl (sat. KCl) were used as an auxiliary and reference electrode and pre-washed GCE (glassy carbon electrode) act as a working electrode.

2.2. Synthesis of Sm_2O_3 nanoparticles

Analytical grade Samarium (III) nitrate hexahydrate (Sm $(NO_3)_3 \cdot 6H_2O$), polyethylene glycol (PEG) and ethanol were obtained from sigma-Aldrich and used without any additional purification. A 1g of $Sm(NO_3)_3 \cdot 6H_2O$ was mixed with 5g of PEG and the mixture was kept into hydrothermal at 150^0 C for 5 h [17]. The acquired precipitate was centrifuged and washed with distilled water followed by ethanol. The synthesized Sm_2O_3 Nanoparticles (NPs) were calcinated at 100^0 C for 2 h.

2.3. Preparation of Sm_2O_3 NPs modified GCE

The 1mg of synthesized Sm_2O_3 NPs was dispersed in 1 ml of water and sonicated for 15 min before drop coating the prepared Sm_2O_3 NPs colloidal the GCE surface was polished three repeated times with 0.5mg of Al_2O_3 slurry. Finally, the 6μL of Sm_2O_3 NPs colloidal were drop-coated on the polished GCE surface and dried at 50^0 C. The prepared Sm_2O_3 NPs/GCE was used for further electrochemical analysis.

3. RESULTS AND DISCUSSION

3.1. FESEM and XRD Sm_2O_3 NPs

The morphological structure of the synthesized nanomaterials was explored using FE-SEM. Fig. 1A-C displays the FESEM image of the Sm_2O_3 NPs with different magnification. In Fig.1A and B,

particles are slightly agglomerates and arranged irregular shape. Further, the magnified FESEM image of the Sm_2O_3 NPs clearly shows that numerous particles are in rhombus like structure as displayed in Fig.1C.

The XRD spectrum of Sm_2O_3 NPs has displayed in Fig.1D. It shows the characteristic diffraction peak at 28.3^0 (222), 32.7^0 (400), 47.0^0 (440), 55.7^0 (622) and 58.45^0 (444). The obtained peaks were corresponding to the standard XRD spectrum of Sm_2O_3 (JCPDS No. 15-0813)[18]. Additionally, the obtained XRD spectrum reveals that synthesized Sm_2O_3 NPs follows the cubic crystal system. The grain size of the synthesized Sm_2O_3 NPs was calculated be 13.70 nm by using the Scherrer equation[19].

$$D = (k\lambda/\beta \cos \theta)$$

Were D being crystalline size of the particle (nm), k is the dimensionless shape factor (0.94), λ is the wavelength of X-Ray (1.54178Å), β was the Full width at half maximum of the diffraction peak (FWHW) and θ is the diffraction angle.
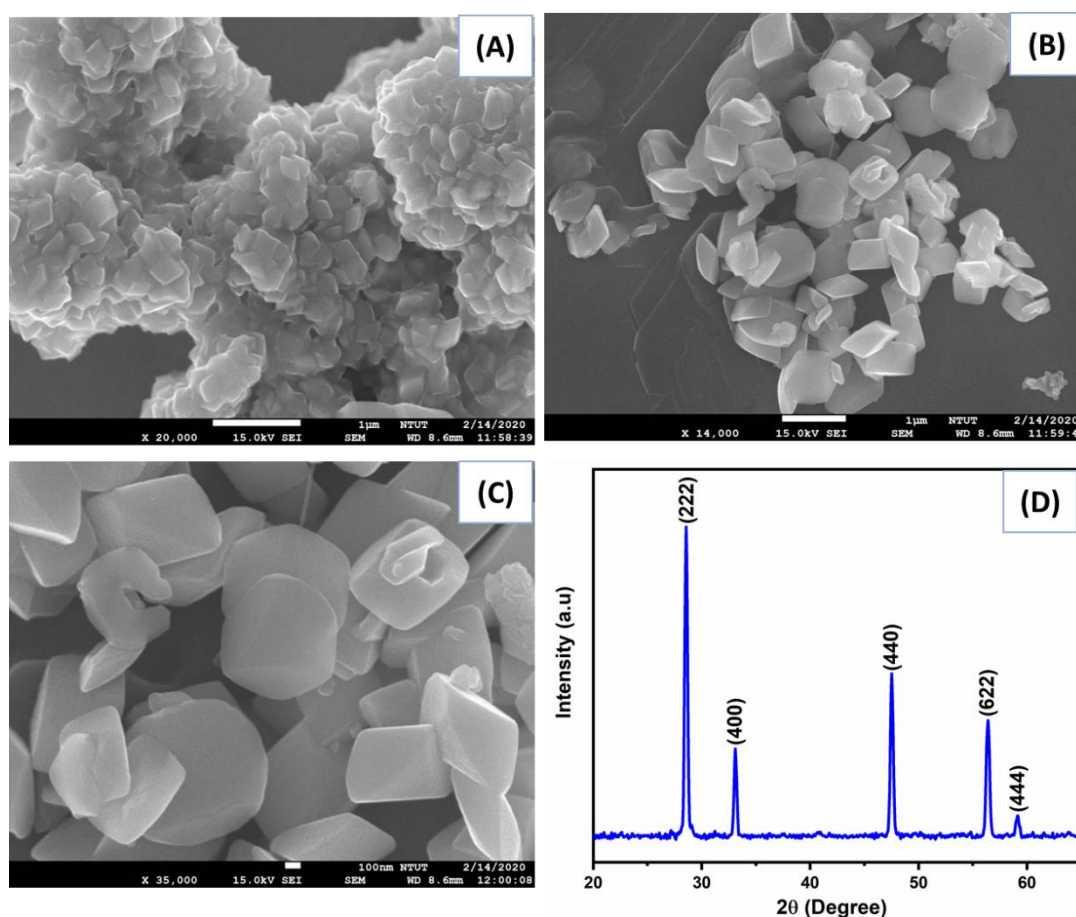

Figure 1. FE-SEM of Sm_2O_3 NPs (A-C) XRD spectrum of Sm_2O_3 (D)

3.2. Electrochemical study of Sm_2O_3 NPs/GCE

Fig.2A displays EIS curve of the bare GCE (a) and Sm_2O_3 NPs/GCE (b) in 0.1 M KCl consist of 0.05M $[Fe(CN)_6]^{3-/4-}$ with frequency range of 100 MHz to 100 KHz. The EIS curve was fitted according

to the Randle's equivalent circuit model shown in the inset Fig.2A. Where, R_{ct}, Z_w, R_s and C_{dl} are charge transfer resistance, Warburg impedance, ohmic resistance and the double layer electron-transfer resistance. The R_{ct} value of bare GCE (a) and Sm_2O_3 NPs/GCE (b) were found to be 337.56 Ω and 87.46 Ω. The Sm_2O_3 NPs/GCE show small R_{ct} because of its large active surface area compared to bare GCE.
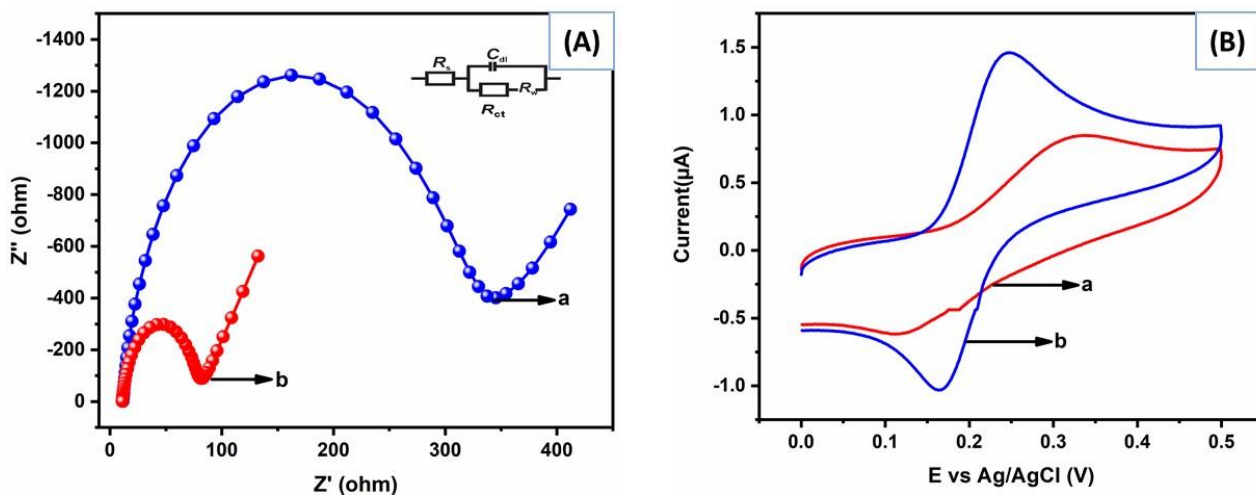

Figure 2. (A) EIS of bare GCE (a) and Sm_2O_3 NPs/GCE (b) (B) CV's of bare GCE (a) and Sm_2O_3 NPs/GCE (b) in presence of 25 µM DA at 0.1 M pH-7

Fig.2B explains the CV's obtained for bare GCE (a) and Sm_2O_3 NPs/GCE (b) at 0.1M pH-7 which consist of 25µM DA at constant scan rate 0.05 Vs^{-1}. The bare GCE shows lowest oxidation peak comparing with Sm_2O_3 NPs/GCE. In addition, Sm_2O_3 NPs modified GCE exhibits an intense oxidation peak with peak current of 1.48µA with minimum oxidation potential of 0.24 V due to the presence of large active area compared with bare GCE. In general dopamine oxidation exhibits in two steps, at first dopamine releasees $2e^-$ and convert into dopamine quinone. Further, it reverts back into dopamine by accepting the $2e^-$ during reversible reduction[20]. Thus, the clear dopamine redox mechanism were established in mechanism 1.
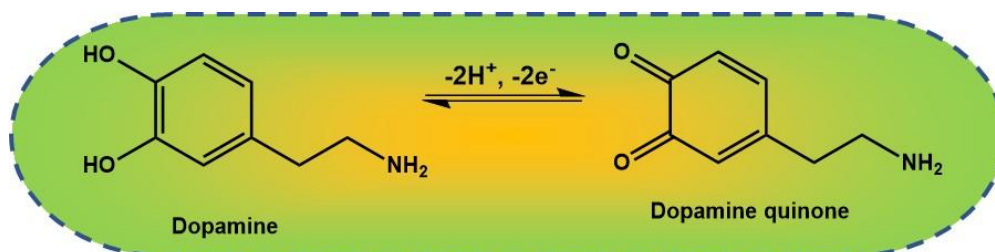
Mechanism 1. The redox mechanism of Dopamine

The effect of change in concentration of DA on Sm_2O_3 NPs/GCE were performed on fixed scan rate of 0.05Vs^{-1} with 0.1M pH-7 was shown on Fig.3A.The concentration was increased from 25µM to 200µM. For every consecutive addition DA the anodic current has raised linearly. Additionally, the

correlation between current vs [DA]/µM has been displayed on the Fig.3B and their regression equation was written as y=0.0383x + 0.3304 with correlation coefficient of R^2= 0.9957 and cathodic as y= -0.0143x – 0.5648 with R^2= 0.9922. The scan rate for DA detection by Sm_2O_3 NPs/GCE was examined by CV technique from 0.02 to 0.2 Vs^{-1} containing 100µM of DA were given in Fig.3C. In addition, the regular increase in scan rate shows a linear increase redox current peak. Fig.3D displays the current obtained for DA versus square root of scan rate. Moreover, the correlation coefficient was found to be R^2= 0.9908 for anodic and 0.997 for cathodic peak with regression equation of y= 17.824x + 0.086 for oxidation and y= -16.059x - 1.5894 for reduction peak current, which shows that oxidation of DA by Sm_2O_3 NPs/GCE were diffusion-controlled process.
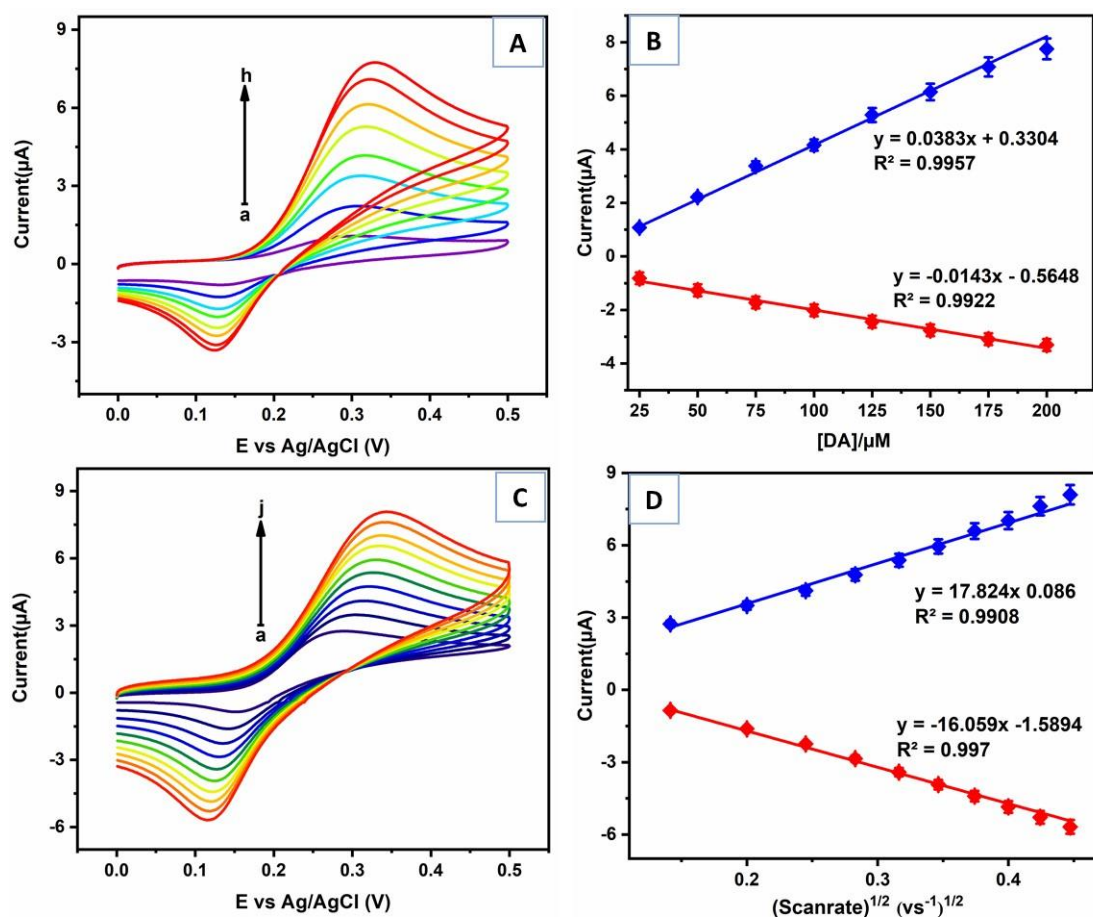

Figure 3. (A) Effect of concentration (a to h-25 to 200µM) DA on Sm_2O_3 NPs/GCE and CVs occurred for Sm_2O_3 NPs/GCE at increasing scan rates (a to j-0.02 to 0.2 Vs^{-1}) (C) in 0.1 M pH-7 containing 100 µM DA. Linear plot for redox current peak Vs DA concentration (B) and square root of scan rate (D).

Differential pulse voltammetry (DPV) oxidation current response peak for the detection of DA has displayed on the Fig.4A. The anodic peak current increase with increase in the concentration of DA in 0.1 M of pH-7. The Sm_2O_3 NPs/GCE has a linear response towards to the electrochemical sensing of DA with a linear range of 0.01 to 342.9 µM and limit of detection to 2.54 nM. Furthermore, the linear

regression equation of y= 0.1045x + 0.1063 with the correlation coefficient of R^2= 0.997 were shown in Fig.4B. This result shows that Sm_2O_3 NPs/GCE exhibits an excellent performance towards the detection of DA.
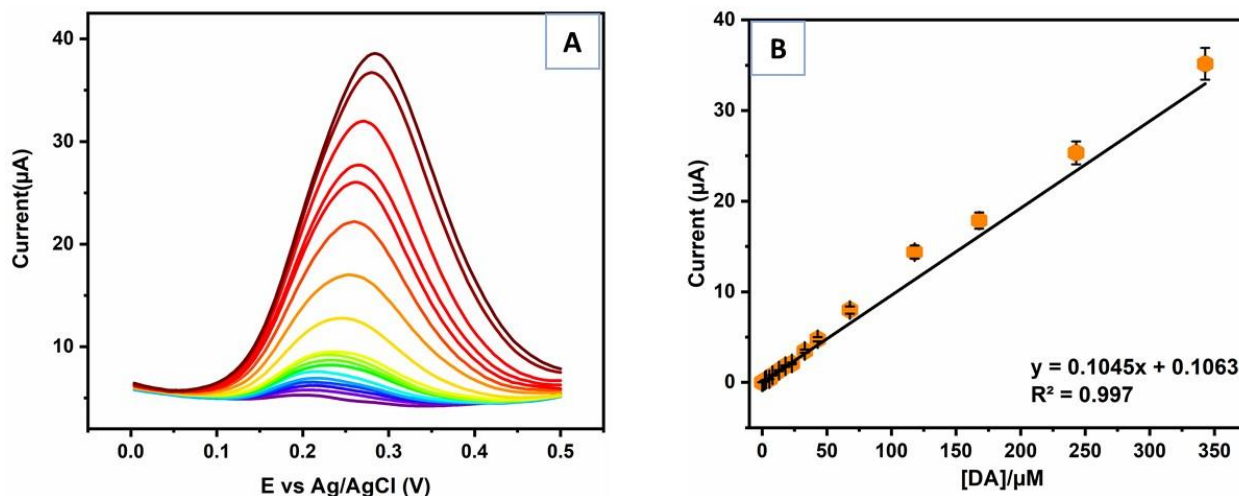

Figure 4. (A) DPV curve for the increasing concentration of DA in 0.1 M pH-7 with respect to Sm_2O_3 NPs/GCE. (B) Linear plot of anodic peak current Vs DA concentration.
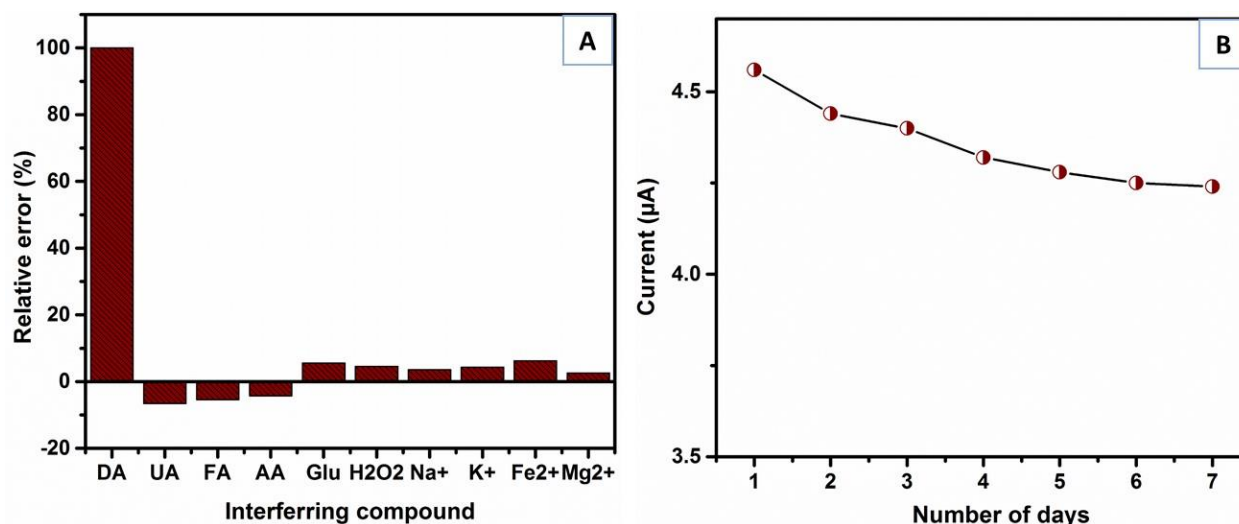

Figure 5. (A) Selective responses of Sm_2O_3 NPs/GCE on 100μM of DA. (B) Stability of Sm_2O_3 NPs/GCE for continuous usage for a week towards 100μM of DA on pH-7.

For an electrochemical sensor, selectivity and stability are the important parameters. The synthesized Sm_2O_3 NPs/GCE was tested for its selectivity using the DPV technique. The Sm_2O_3 NPs/GCE were tested for DA detection with the presence of 5 folds of higher possible interferons like uric acid (UA), folic acid (FA), ascorbic acid (AA), glucose (Glu), H_2O_2, and continued to the 10 folds of Na^+, K^+, Fe^{2+}, Mg^{2+} were given in the Fig.5A. As the results, the prepared sensors shows the relative error with less than 6 %, which clearly shows that synthesized Sm_2O_3 NPs/GCE exhibit an specific selectivity towards the detection of DA. Moreover, Fig.5B shows the working stability of Sm_2O_3

NPs/GCE examined with 0.1 M of pH-7 containing 100μM of DA for a week and after every use the electrode was stored at 4^0 C. The electrode showed 94.5% of its initial current response. Therefore, it confirms that Sm_2O_3 NPs/GCE has an excellent stability towards DA sensing.

Table 1. Comparative studies of DA detection by Sm_2O_3 NPs/GCE with different electrodes from the earlier reports

Method	Linear range ($\mu mol\ L^{-1}$)	LOD ($\mu mol\ L^{-1}$)	Ref
[a]CuTRZMoO$_4$/PPy/[b]GCE/[c]DPV	1 to 100	0.8	[21]
[d]Ni$_{3-x}$Te$_2$/[e]CPE/[f]SWV	4 to 31	0.15	[22]
[g]Co-Ni Hs/[b]GCE/[c]DPV	10 to 500	8.2	[23]
[h]2,6 DAP-ERGO/MoO$_3$/[b]GCE/[c]DPV	0.1 to 900	0.025	[24]
[i]AuNBP/MWCNTs/[b]GCE/[c]DPV	0.05 to 2700	0.015	[25]
[j]ACCG/Nafion/[b]GCE /[k]it-Amp	0.1 to 50	0.1	[26]
[l]Pt-CNC/MWCNT/GO/[b]GCE/[c]DPV	0.8 to 300	0.27	[27]
[m]MnO/C/[b]GCE/[f]SWV	0.2 to 10	0.009	[28]
Sm$_2$O$_3$/GCE/DPV	0.01 to 342.9	0.00254	**[This work]**

[a]- Molybdenum oxide-based metal-organic framework/polypyrrole
[b]- Glassy carbon electrode
[c]- Differential pulse voltammetry
[d]- Nickel telluride
[e]- Carbon paste electrode
[f]- Square wave voltammetry
[g]- Cobalt-nickel hollow spheres
[h]- 2, 6 diaminopyridine functionalized electrochemically reduced graphene oxide with molybdenum oxide ternary composites
[i]- Gold nanobipyramid/multi-walled carbon nanotube hybrids
[j]- Sliver doped dual-phase copper oxide containing g-C_3N_4
[k]- it-Amperometric
[l]- Platinum concave nanocubes loaded on multiwall carbon nanotubes and graphene oxide nanocomposite
[m]- MnO nanoparticles were coated by sheet-like carbon

3.3. Real sample analysis of Sm₂O₃ NPs/GCE

DPV techniques was subjected to investigate the practical application of the prepared sensor in the biologic samples including human blood serum and urine samples. The biologic samples was brought from the Chang-Gung memorial hospital, Taiwan. Then, the collected serum and urine samples were diluted with buffer solution and the known concentration of DA was spiked. Furthermore, under the optimized conditions the spiked samples was tested for its practical applicability. As the results, Sm_2O_3

NP$_S$/GCE provide the owing found and recovery values, which are tabulated in table 2. In the end, the prepared Sm$_2$O$_3$ NPs/GCE established as an effective electrode for the practical applicability.

Table 2. Real sample analysis of DA in spiked human blood serum and urine samples on Sm$_2$O$_3$ NPs/GCE

Real Samples	Added/ nM	Found/ nM	Recovery/%	*RSD/% (n=3)
Human Serum samples	50.00	48.85	97.70	3.51
	100.00	96.52	96.52	3.24
	200.00	192.50	96.28	3.45
Urine samples	100.00	97.08	97.08	2.77
	200.00	188.64	94.32	3.19
	300.00	291.42	97.14	2.86

* Related standard deviation (RSD).

4. CONCLUSION

In summary, Sm$_2$O$_3$ NPs was successfully synthesized using the hydrothermal method. The microscopic and XRD studies confirms the well dispersion of Sm$_2$O$_3$ NPs. Further, Sm$_2$O$_3$ NPs modified electrode possessed the excellent electrochemical activity for the detection of dopamine. Moreover, the Sm$_2$O$_3$ NPs modified electrode precisely enhanced the sensitivity as the results the proposed sensor exhibited good covering range of 0.01 to 342.9 µM, with the detection limit of 2.54 nM. Besides, the Sm$_2$O$_3$ NPs/GCE also possessed the higher selectivity, and outstanding storage stability for the detection of dopamine. In addition, the real time analysis of the as synthesized nanoparticle were examined in the spiked serum and urine samples, which shows the good recovery for both samples. To our knowledge, the as synthesized Sm$_2$O$_3$ NPs is one of the most efficient electrode material for the DA sensing.

Reference

1. R. Zhang, G.-D. Jin, D. Chen, X.-Y. Hu, *Sens. Actuators, B*, 138 (2009) 174-181.
2. Y. Huang, Y. Tang, S. Xu, M. Feng, Y. Yu, W. Yang, H. Li, *Anal. Chim. Acta*, 1096 (2020) 26-33.
3. S. Kogularasu, M. Akilarasan, S.-M. Chen, T.-W. Chen, B.-S. Lou, *Mater. Chem. Phys.,* 227 (2019) 5-11.
4. L. Zhihua, Z. Xucheng, W. Kun, Z. Xiaobo, S. Jiyong, H. Xiaowei, M. Holmes, *Innovative Food Sci. Emerg. Technol.,* 31 (2015) 196-203.
5. D. Li, P.C. Sham, M.J. Owen, L. He, *Hum. Mol. Genet.,* 15 (2006) 2276-2284.

6. L. Yang, D. Liu, J. Huang, T. You, *Sens. Actuators, B*, 193 (2014) 166-172.
7. M. Moccia, S. Pappatà, R. Erro, M. Picillo, C. Vitale, M. Amboni, K. Longo, R. Palladino, P. Barone, M.T. Pellecchia, *Acta Neurol. Scand.,* 131 (2015) 127-131.
8. V. Mani, T.-W. Chen, S. Selvaraj, *Int. J. Electrochem. Sci.,* 12 (2017) 7446-7456.
9. V. Mani, T.-W. Chen, S. Selvaraj, *Int. J. Electrochem. Sci.,* 12 (2017) 7435-7445.
10. V. Mani, M. Govindasamy, S.-M. Chen, B. Subramani, A. Sathiyan, J.P. Merlin, *Int. J. Electrochem. Sci.,* 12 (2017) e267.
11. S. Maheshwaran, M. Akilarasan, S.-M. Chen, T.-W. Chen, E. Tamilalagan, C.Y. Tzu, B.-S. Lou, *J. Electrochem. Soc.,* 167 (2020) 066517.
12. E. Elaiyappillai, M. Akilarasan, S.-M. Chen, S. Kogularasu, P.M. Johnson, E.B. Tamilarasan, *J. Electrochem. Soc.,* 167 (2020) 027544.
13. J. Gao, Y. Zhao, W. Yang, J. Tian, F. Guan, Y. Ma, J. Hou, J. Kang, Y. Wang, *Mater. Chem. Phys.,* 77 (2003) 65-69.
14. B. Mutharani, S. Sakthinathan, S.-M. Chen, T.-W. Chen, T.-W. Chiu, *Int. J. Electrochem. Sci.,* 13 (2018) 6996-7007.
15. A.S. Dezfuli, M.R. Ganjali, H.R. Naderi, *Appl. Surf. Sci.,* 402 (2017) 245-253.
16. M. Rahimi-Nasrabadi, S.M. Pourmortazavi, M. Aghazadeh, M.R. Ganjali, M.S. Karimi, P. Novrouzi, *J. Mater. Sci. - Mater. Electron.,* 28 (2017) 5574-5583.
17. S. Biswas, H. Naskar, S. Pradhan, Y. Chen, Y. Wang, R. Bandyopadhyay, P. Pramanik, *New J. Chem.,* (2020).
18. R. Mohammadinasab, M. Tabatabaee, H. Aghaie, M.A. Seyed Sadjadi, *Synth. React. Inorg. Met.-Org. Chem.,* 45 (2015) 451-454.
19. S.P. Ghorpade, R. Harikrishna, R.M. Melavanki, V. Dubey, N. Patil, *Optik,* (2020) 164533.
20. S. Cheemalapati, S. Palanisamy, V. Mani, S.-M. Chen, *Talanta,* 117 (2013) 297-304.
21. K. Zhou, D. Shen, X. Li, Y. Chen, L. Hou, Y. Zhang, J. Sha, *Talanta,* 209 (2020) 120507.
22. K. de Fatima Ulbrich, J.P. Winiarski, C.L. Jost, C.E.M. de Campos, *Compos. B. Eng.,* 183 (2020) 107649.
23. C. Yang, X. Sun, C. Zhang, M. Liu, *J. Nanopart. Res.,* 22 (2020) 1-7.
24. N. Roy, S. Yasmin, S. Jeon, *Microchem. J.,* 153 (2020) 104501.
25. J. Cheng, X. Wang, T. Nie, L. Yin, S. Wang, Y. Zhao, H. Wu, H. Mei, *Anal. Bioanal. Chem.,* (2020) 1-9.
26. A. Verma, S. Kumar, W.-K. Chang, Y.-P. Fu, *Dalton Trans.,* (2020).
27. X. Zhang, J. Zheng, *Talanta,* 207 (2020) 120296.
28. L. Xiao, L. Jia, S. Zhao, X. Tang, C. Zhu, H. Huang, J. Jiang, M. Li, *J. Electroanal. Chem.,* (2020) 113823